Journal of Highway and Transportation Research and Development
2024, 18(1): 38-45
ISSN 2095-6215
DOI: 10.26599/HTRD.2024.9480005

# Lateral Control of Autonomous Vehicles with Data Dropout via an Enhanced Data-driven Model-free Adaptive Control Algorithm

Shida Liu*, Yuhao Yan, Honghai Ji**, Li Wang

(School of Electrical and Control Engineering, North China University of Technology, Beijing 100093, China)

**Abstract**: Addressing the lateral path tracking control issue of autonomous vehicles during data dropout, an improved model-free adaptive control system with data compensation (DC-EMFAC) is introduced. First, the method introduces a dynamic linearization technique with a time-varying factor pseudo gradient (PG) to linearize the dynamic process of an autonomous vehicle, and then designs a model-free adaptive controller. Moreover, addressing the issue of data dropout in the actual system, this paper employs an estimation algorithm to estimate the data loss at the present time based on the system's input and output (I/O) from the past and PG. The advantage of the DC-EMFAC is that the controller design process is based on the I/O data of the controlled object, without the need for an accurate mathematical model. The effectiveness of the proposed algorithm is verified through a series of simulations on the Panosim platform.

**Key words**: automotive engineering; autonomous vehicle; model-free adaptive control (MFAC); data dropout; data compensation; data driven control

## 1 Introduction

Recently, with the development of control field, it has provided a solid theoretical basis for the field of self-driving technology. Therefore, intelligent control for automobiles has become one of the hottest control research issues. However, in the actual road, the driving path of the autonomous vehicle is complex and changeable, which makes it necessary for the autonomous vehicle to track the vehicle in front to ensure its own travel safety under certain special circumstances, which has new requirements for the lateral path tracking of the autonomous vehicle, especially considering the existence of data loss in the actual situation.

At present, many data dropout with compensation controllers have been designed. On the problem that Bernoulli random variable modeling has random data loss in iterative learning control, two schemes to deal with random data loss are proposed[1]. For uncertain Takagi-Sugeno fuzzy system, based on Lyapunov function method, the controller is improved by introducing FMF function to compensate for data dropout[2]. The H-infinity control problem on networks with data loss, and the non-convex feasible problem is solved by CCL method[3].

However, the abovementioned control algorithms are based on accurate models. Because the process of establishing an accurate model is very complex in practical application, the simplified model is not comprehensive enough to describe controlled object. Meanwhile, the MFAC algorithm complete the design of the controller only rely on the I/O data of the controlled object without establish accurate mathematical model. MFAC has been used in many engineering cases. A controller design based on DuSP-MFAC is proposed to the lateral tracking of autonomous vehicle[4]. A model-free adaptive data dropout control algorithm based on dynamic linearization of compact form is proposed[5]. A cCMFAILC control algorithm is proposed and applied to the cooperative control of multiple metro trains under data dropout[6].

Aiming at the problem of data dropout in autonomous vehicle's lateral path tracking. The main contributions are as follows:

(1) The DC-EMFAC algorithm is designed for the lateral control problem of autonomous vehicle in the case of data dropout. Firstly, the autonomous vehicle system is dynamically linearized, and a time-varying pseudo gradient (PG) vector is used to make the algorithm adaptive. A data compensation algorithm is adopted when da-

Received 15 March 2023; Revised 19 July 2023; Accepted 26 July 2023

* *E-mail address*: lsdshiwo@hotmail.com

** Corresponding author, jhh@ncut.edu.cn

ta is lost, then the compensated data is used to control the controlled object to achieve the desired goal. The advantage of the proposed algorithm is that not only does the controller utilize the I/O data of the controlled object, but also it can handle control problem in the event of data dropout.

(2) A series of simulations were carried out by using Panosim platform and MATLAB 2018b, and the tracking performance of DC-EMFAC and MFAC with partial form dynamic linearization (PFDL-MFAC) are compared under the condition of data dropout. It can be verified that the DC-EMFAC method used has excellent control effect in the lateral control of the autonomous vehicle.

The structure of this paper is as follows: In the second chapter, through analysis the lateral dynamics of the autonomous vehicle, the preview-deviation-yaw (PDY) of the control target is defined. Moreover, DC-EMFAC algorithm is proposed and applied to address the issue of the lateral path tracking control of autonomous vehicle under data dropout. In the third chapter, a series of simulations are carried out in Panosim to verify the feasibility of DC-EMFAC algorithm. The last chapter summarizes the key findings of this study and explores its potential future applications and implications.

## 2 Design of lateral tracking controller for autonomous vehicle

### 2.1 Dynamics analysis of autonomous vehicle

The path tracking of autonomous vehicle has been a relatively complex control problem. In order to analyze the autonomous vehicle more clearly, establishing its dynamic model is a relatively simple and easy way to implement in engineering[7].

The lateral path tracking problem of autonomous vehicle with data loss is studied in depth by dynamic model of autonomous vehicle. The controlled object can be abstracted as a SISO system. Based on the research objectives and problems solved, the tracked vehicle in front is defined as the Look-ahead point, and the preview distance is defined as the length of the line between the point on the target path of the tracked vehicle with the smallest length from the current position and the Look-ahead point[4,8]. The process is shown in Figure 1.

In Figure 1, $\delta$ is the heading angle of the controlled

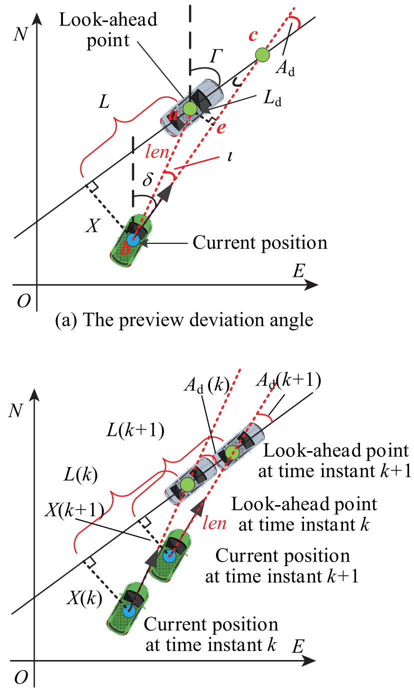


(a) The preview deviation angle

(b) Lateral tracking control

**Fig. 1 Schematic diagram of lateral dynamics analysis**

object, $\Gamma$ is the heading angle of the tracked vehicle, $L$ is the preview distance, $L_d$ is the vertical distance, $A_d$ is the angle deviation. Denote the included angle between the vehicle movement direction and this line as $\iota$, and define this included angle as PDY. It is specified that the Look-ahead point is negative when it is on the left of the autonomous vehicle, and positive when it is on the right[9].

Equation (1) can be got from Figure 1:

$$\iota = \arctan \frac{X}{l} - A_d \tag{1}$$

Considering the actual situation, the controlled object can be expressed as the following nonlinear system[10]:

$$\iota(k+1) = f[\iota(k),\cdots,\iota(k-n_\nu), q(k),\cdots,q(k-n_\kappa)], \tag{2}$$

where, $q(k)$ is denote as steering wheel angle; $f(\cdots)$ is an unknown system; $n_\kappa, n_\nu$ represent the order of system input and output.

Assume that the position coordinate of the current autonomous vehicle is $(x^*, y^*)$, and the position coordinate of the Look-ahead point is $(x^*, y^*)$, denote $dx = x - x^*$, $dy = y - y^*$. In order to prevent $dy = 0$ causing the algorithm to fail to run, a very small positive number $\psi$ is used to calculate the PDY:

$$\iota(\mathrm{d}x,\mathrm{d}y,\vartheta)=\begin{cases} f_{pi}[\arctan(\mathrm{d}x/\mathrm{d}y)-\vartheta], \\ \text{if } \mathrm{d}x\geqslant 0,\ \mathrm{d}y>\psi \\ f_{pi}[\arctan(\mathrm{d}x/\mathrm{d}y)-\vartheta], \\ \text{if } \mathrm{d}x\leqslant 0,\ \mathrm{d}y>\psi \\ f_{pi}[\arctan(\mathrm{d}x/\mathrm{d}y)+\pi-\vartheta], \\ \text{if } \mathrm{d}x\geqslant 0,\ \mathrm{d}y<-\psi \\ f_{pi}[\arctan(\mathrm{d}x/\mathrm{d}y)-\pi-\vartheta], \\ \text{if } \mathrm{d}x\leqslant 0,\ \mathrm{d}y<-\psi \\ f_{pi}(\pi/2-\vartheta), \\ \text{if } \mathrm{d}x\geqslant 0,\ -\psi\leqslant \mathrm{d}y\leqslant\psi \\ f_{pi}(\pi/2-\vartheta), \\ \text{if } \mathrm{d}x\leqslant 0,\ -\psi\leqslant dy\leqslant\psi \end{cases}, \quad (3)$$

where, $\vartheta$ is the starting coordinate direction. Denote the due north direction is 0 radian; $f_{pi}$ is a limiting function to limit the monitored angle to the range of $(-\pi,\pi)$. $f_{pi}$ can be described as:

$$f_{pi}(\chi)=\begin{cases}\chi-2\pi, & \chi>\pi \\ \chi, & \pi>\chi>-\pi, \\ \chi+2\pi, & \chi<-\pi\end{cases} \quad (4)$$

where $\chi$ is the independent variable of function $f_{pi}(\chi)$.

## 2.2 Controller design

### 2.2.1 Dynamic linearization

Through the previous dynamics analysis of autonomous vehicle, it can be determined that in the lateral tracking problem, the goal is to control the *PDY* around zero.

The lateral control system of autonomous vehicle can be regarded as a time discrete nonlinear system of SISO[11], it can be expressed as formula (2).

Denote $\boldsymbol{Q}_\xi(k)\in R^L$ composed of all control input data at $L$ moment, it can be got:

$$\boldsymbol{Q}_\xi(k)=[q(k),\cdots,q(k-\xi+1)]^{\mathrm{T}}. \quad (5)$$

$\boldsymbol{Q}_\xi(k)=\boldsymbol{0}_\xi$ when $k\leqslant 0$, $\xi$ is control input linearization length.

Assumption 1: $f(\cdots)$ has the continuous partial derivatives from $(n_y+2)$ variable to $(n_y+\xi+1)$ variable.

Assumption 2: For any $k_1\neq k_2$, $k_1,k_2\geqslant 0$ and $\boldsymbol{Q}_\xi(k_1)\neq\boldsymbol{Q}_\xi(k_2)$, system (2) satisfies the generalized Lipschitz condition and it has: $|\iota(k_1+1)-\iota(k_2+1)\|b\|\boldsymbol{Q}_\xi(k_1)-\boldsymbol{Q}_\xi(k_2)\|$, and $\iota(k_i+1)=f[\iota(k_j),\cdots,\iota(k_j-n_y),q(k_j),\cdots,q(k_j-n_u)]$, $j=1,2,\cdots$. $b$ is a constant and satisfied $b>0$. Denote $\Delta\boldsymbol{Q}_\xi(k)=\boldsymbol{Q}_\xi(k)-\boldsymbol{Q}_\xi(k-1)$.

Lemma 1: For the nonlinear system satisfying Assumption 1 and Assumption 2, when $\xi$ has constant value and $\|\Delta\boldsymbol{Q}_\xi(k)\|\neq 0$, there has a vector named Pseudo Gradient (PG) satisfied $\boldsymbol{\phi}_{P,\xi}(k)\in R^L$, which make SISO system can be converted into data model:

$$\Delta\iota(k+1)=\boldsymbol{\phi}^{\mathrm{T}}_{P,\xi}(k)\Delta\boldsymbol{Q}_\xi(k), \quad (6)$$

where $\boldsymbol{\phi}^{\mathrm{T}}_{P,\xi}(k)=[\phi_1(k),\cdots,\phi_\xi(k)]^{\mathrm{T}}$ is bounded for any $k$[14].

### 2.2.2 Control algorithm design

For the following criteria functions:

$$H(q(k))=[\iota^*(k+1)-\iota(k+1)]^2+\lambda[q(k)-q(k-1)]^2, \quad (7)$$

where $\lambda$ is a weighting factor and $\lambda>0$.

Take equation (6) into equation (7), take the derivative of $q(k)$, then make it equal to 0, it can be obtained:

$$q(k)=q(k-1)+\frac{\rho_1\phi_1(k)[\iota^*(k+1)-\iota(k)]}{\lambda+|\phi_1(k)|^2}-\frac{\phi_1(k)\sum_{j=2}^{\xi}\rho_j\phi_j(k)\Delta q(k-j+1)}{\lambda+|\phi_1(k)|^2}, \quad (8)$$

where, $\iota^*(k+1)$ is the desired PDY at $k+1$ moment; $\rho_j$ is the step factor and $\rho_j\in(0,1]$, $(j=1,2,\cdots,\xi)$.

Because the true value of *PG* in the controller cannot be obtained, this paper uses a projection algorithm to estimate *PG* as follow:

$$H[\phi_{P,\xi}(k)]=|\iota(k)-\iota(k-1)-\boldsymbol{\phi}^{\mathrm{T}}_{P,\xi}(k)\Delta\boldsymbol{Q}_\xi(k-1)|^2+\mu\|\boldsymbol{\phi}_{P,\xi}(k)-\hat{\boldsymbol{\phi}}_{P,\xi}(k-1)\|^2, \quad (9)$$

where $\mu$ is the weighting factor and $\mu>0$.

Equation (9) finds the extreme value of $\boldsymbol{\phi}_{P,\xi}(k)$ to obtain the *PG* estimation algorithm:

$$\hat{\boldsymbol{\phi}}_{P,\xi}(k)=\hat{\boldsymbol{\phi}}_{P,\xi}(k-1)+\frac{\eta\Delta\boldsymbol{Q}_\xi(k-1)[\iota(k)-\iota(k-1)-\hat{\boldsymbol{\phi}}^{\mathrm{T}}_{P,\xi}(k-1)\Delta\boldsymbol{Q}_\xi(k-1)]}{\mu+\|\Delta\boldsymbol{Q}_\xi(k-1)\|^2}, \quad (10)$$

where, $\eta\in(0,2)$; $\hat{\boldsymbol{\phi}}^{\mathrm{T}}_{P,\xi}$ is the estimated value of $\boldsymbol{\phi}^{\mathrm{T}}_{P,\xi}$; In order to make the *PG* have strong ability of time-varying parameter tracking, a reset algorithm is used:

$$\begin{cases}\hat{\boldsymbol{\phi}}_{P,\xi}(k)=\hat{\boldsymbol{\phi}}_{P,\xi}(1) \\ \text{if} \quad \|\hat{\boldsymbol{\phi}}_{P,\xi}(k)\|\leqslant\varepsilon \text{ or } \|\Delta\boldsymbol{Q}_\xi(k-1)\|\leqslant\varepsilon\end{cases}, \quad (11)$$

where $\varepsilon$ is a minimal positive number.

Considering the existence of data dropout in actual engineering practice, due to the interference of various unstable factors inside and outside the system, the data monitored by the sensor may not match the actual situation or the data loss may cause the controller to fail to follow the expected target to work[15]. In order to deal with this situation, this paper makes the following improvements to the PFDL-MFAC algorithm when data dropout occurs:

$$\check{\iota}(k)=\begin{cases}\iota(k),\ \mathrm{sign}(k)=1\\ \Omega\times\check{\iota}(k-1)+(1-\Omega)\\ \quad[\check{\iota}(k-1)+\boldsymbol{\phi}_{P,\xi}^{\mathrm{T}}(k-1)\\ \quad\Delta\boldsymbol{Q}_{\xi}(k-1)),\ \mathrm{sign}(k)=0\end{cases},\tag{12}$$

where, $\mathrm{sign}(k)\in[0,1]$ is a binary variable, which is used to monitor whether the data obtained by the sensor of the system is abnormal; $\Omega$ as a scale factor satisfied $\Omega\in(0,1)$; $\iota(k)$ is the data monitored during normal sensor operation; $\check{\iota}(k)$ is the output after determining whether data dropout has occurred. When data is lost, make $\mathrm{sign}(k)=0$, use the compensated data to control the system. When the sensor operates normally, make $\mathrm{sign}(k)=1$, the actual monitored data is used to control the controlled object.

The operation flow chart is shown in Figure 2.

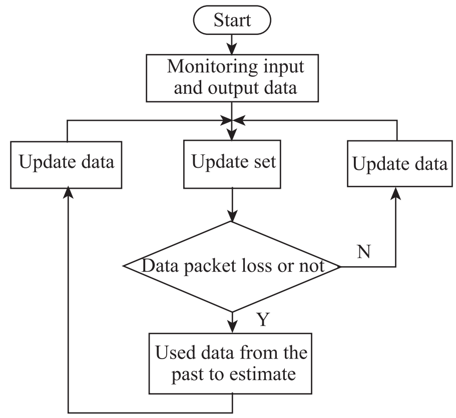


**Fig. 2 Data dropout algorithm operation**

To sum up, take $\check{\iota}(k+1)$ to replace $\iota(k+1)$ in control algorithm (8) and (10), and obtain SISO partial form DC-EMFAC algorithm:

$$\begin{cases}\check{\iota}(k)=\begin{cases}\iota(k),\ \mathrm{sign}(k)=1\\ \Omega\times\check{\iota}(k-1)+(1-\Omega)[\check{\iota}(k-1)+\boldsymbol{\phi}_{P,\xi}^{\mathrm{T}}(k-1)\Delta\boldsymbol{Q}_{\xi}(k-1)],\ \mathrm{sign}(k)=0\end{cases}\\ \hat{\boldsymbol{\phi}}_{P,\xi}(k)=\hat{\boldsymbol{\phi}}_{P,\xi}(k-1)+\dfrac{\eta\Delta\boldsymbol{Q}_{\xi}(k-1)[\check{\iota}(k)-\check{\iota}(k-1)-\hat{\boldsymbol{\phi}}_{P,\xi}^{\mathrm{T}}(k-1)\Delta\boldsymbol{Q}_{\xi}(k-1)]}{\mu+\|\Delta\boldsymbol{Q}_{\xi}(k-1)\|^2}\\ \hat{\boldsymbol{\phi}}_{P,\xi}(k)=\hat{\boldsymbol{\phi}}_{P,\xi}(1),\ \text{if}\ \|\hat{\boldsymbol{\phi}}_{P,\xi}(k)\|\leqslant\varepsilon\ \text{or}\ \|\Delta\boldsymbol{Q}_{\xi}(k-1)\|\leqslant\varepsilon\\ q(k)=q(k-1)+\dfrac{\rho_1\phi_1(k)[\iota^*(k+1)-\check{\iota}(k)]}{\lambda+|\phi_1(k)|^2}-\dfrac{\phi_1(k)\sum_{j=2}^{\xi}\rho_j\phi_j(k)\Delta q(k-j+1)}{\lambda+|\phi_1(k)|^2}\end{cases}\tag{13}$$

The structure diagram of the controller is as follows Figure 3.

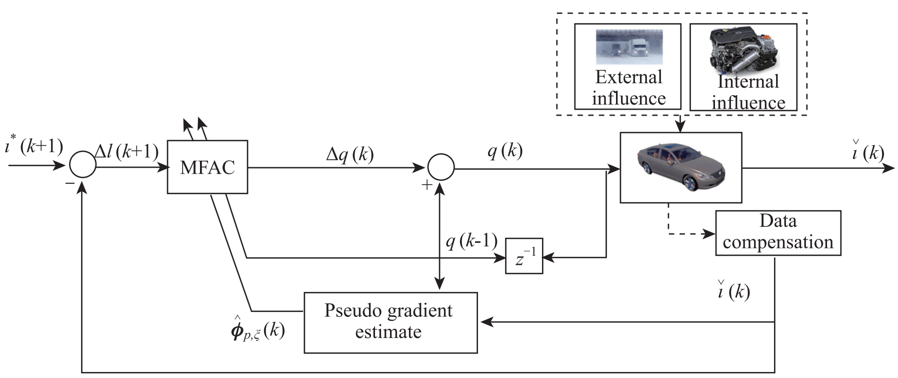


**Fig. 3 Controller structure diagram**

## 3 Simulation analysis

This chapter conducts a series of simulations on the Panosim platform to verify the availability of the DC-EMFAC algorithm and the practicability of the algorithm in the lateral tracking and data loss control of autonomous vehicle[16-17]. The output data were used to draw and analyze in MTALAB2018b. The vehicle and path information in Panosim is shown in Figure 4. Firstly, through debugging the parameters, the control effects of the algorithms with different parameters are compared and the optimal parameters are found. Secondly, the DC-EMFAC algorithm and the PFDL-MAFC algorithm are simulated under different data loss rates, and the control effects of the algorithm are verified. Finally, the applicability of the proposed algorithm in different situations was verified through comparative experiments of different longitudinal speeds.

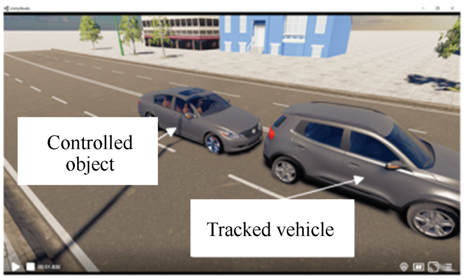


(a) Autonomous vehicle simulation model

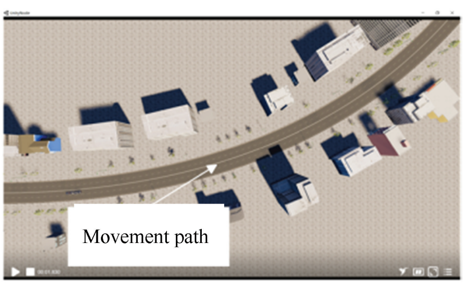


(b) Vehicle movement path

**Fig. 4 Panosim simulation information**

### 3.1 Different weighting factor λ impact on algorithm performance

For the DC-EMFAC controller, its weight factor $\lambda$ has a huge impact on the performance of the algorithm, in order to ensure that the optimal weight factor can be found, a series of simulation have been carried out. The data dropout rate in this section is set to 2%. See Table 1 for parameter selection. Since only considers the lateral tracking of vehicles, the longitudinal speed is always maintained at 20 km/h and $\Omega$=0.2.

Simulate according to different parameters selected in Table 1, and collect the output data of the autonomous vehicle, and get the image as shown in Figure 5.

**Table 1 Different weighting factors λ selection**

| | $\eta$ | $\mu$ | $\rho_i$ | $\lambda$ | $\xi$ |
|---|---|---|---|---|---|
| Scenario 1 | 1 | 0.1 | $\rho_1=1$, $\rho_2=0.6$, $\rho_3=0.4$, $\rho_4=0.2$ | 0.1 | 4 |
| Scenario 2 | 1 | 0.1 | $\rho_1=1$, $\rho_2=0.6$, $\rho_3=0.4$, $\rho_4=0.2$ | 1 | 4 |
| Scenario 3 | 1 | 0.1 | $\rho_1=1$, $\rho_2=0.6$, $\rho_3=0.4$, $\rho_4=0.2$ | 10 | 4 |

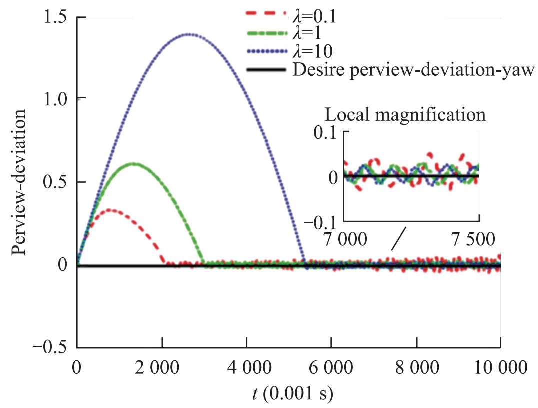


(a) Different λ impact on algorithm tracking performance

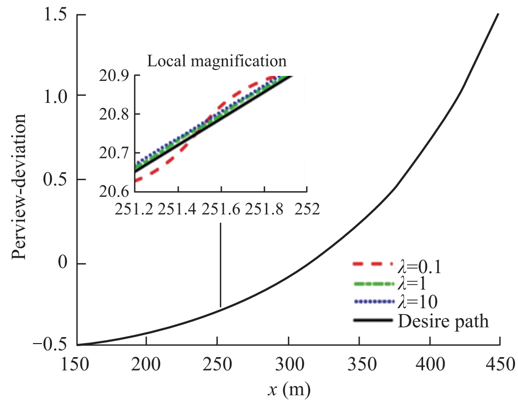


(b) Autonomous vehicle movement path

**Fig. 5 Simulations data**

Through the analysis of Figure 5 and Table 2, it can be found that the response time will be faster when $\lambda$ decreases ($\lambda=0.1$), but there is a large error with the desired goal, the tracking effect of the desired output becomes worse. With the increase of $\lambda$ ($\lambda=10$), the adjustment time of the system becomes longer. When $\lambda=1$ the system can track the desired output in a relatively fast time with a low error. In this simulation, $\lambda=1$ is the best case.

**Table 2 Root-mean-square-errors of PDY**

| | $\lambda$ | Root-mean-square-errors |
|---|---|---|
| Scenario 1 | 0.1 | 0.041 9 |
| Scenario 2 | 1 | 0.018 0 |
| Scenario 3 | 10 | 0.034 5 |

## 3.2 Comparative simulation of different control algorithms with different data dropout rates

DC-EMFAC algorithm and PFDL-MFAC algorithm are compared under different data loss rates. The relevant parameters are shown in Table 3.

**Table 3 Parameter selection**

| | $\eta$ | $\mu$ | $\rho_i$ | $\lambda$ | $\xi$ |
|---|---|---|---|---|---|
| DC-EMFAC | 1 | 0.1 | $\rho_1=1$, $\rho_2=0.6$, $\rho_3=0.4$, $\rho_4=0.2$ | 1 | 4 |
| PFDL-MFAC | 1 | 0.1 | $\rho_1=1$, $\rho_2=0.6$, $\rho_3=0.4$, $\rho_4=0.2$ | 0.01 | 4 |

For different data dropout rates, the simulation results using the above data are as follows Figure 6, Figure 7, Table 4.

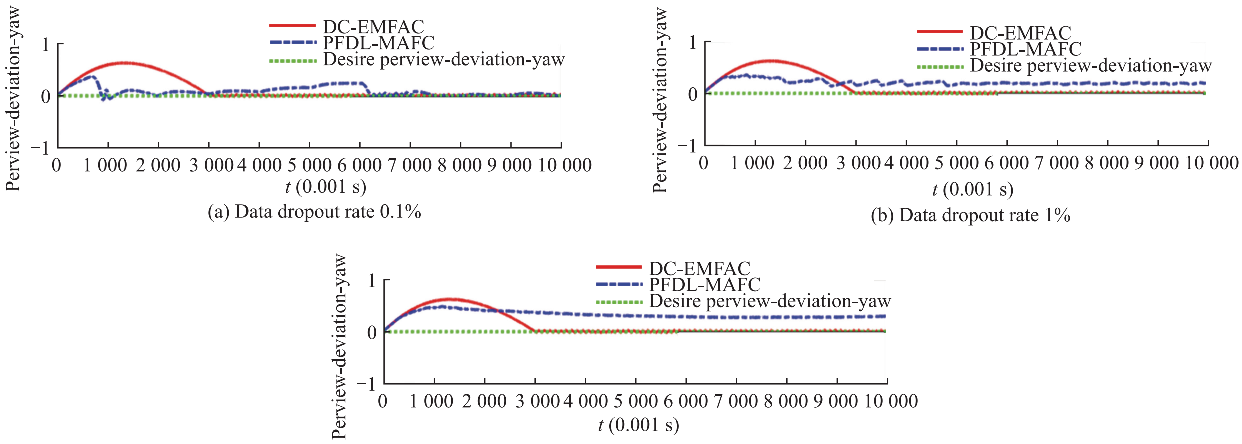

(a) Data dropout rate 0.1%
(b) Data dropout rate 1%
(c) Data dropout rate 2%

**Fig. 6 Control effect under data dropout of different algorithms**

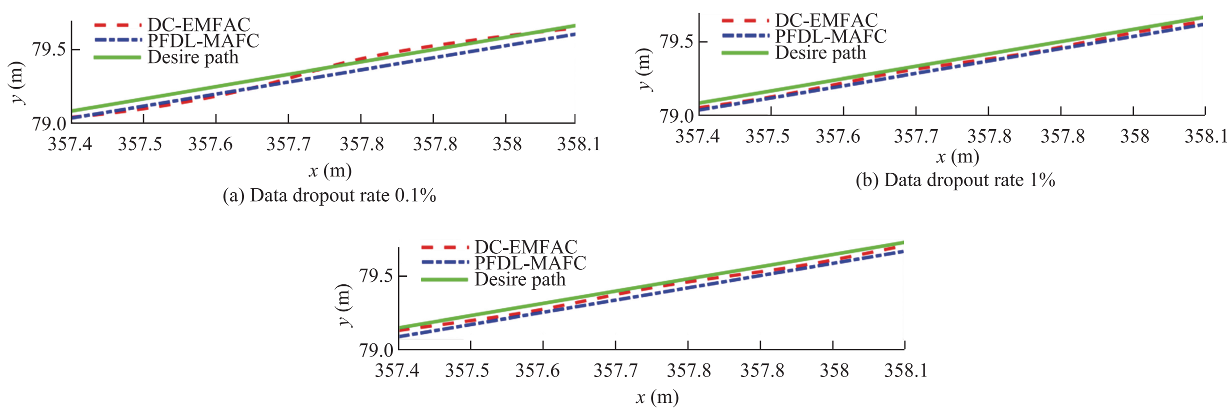

(a) Data dropout rate 0.1%
(b) Data dropout rate 1%
(c) Data dropout rate 2%

**Fig. 7 Autonomous vehicle movement path of different algorithms**

**Table 4 Root-mean-square-errors of PDY in different algorithm**

| Data dropout rate (%) | Root-mean-square-errors of DC-EMFAC | Root-mean-square-errors of PFDL-MFAC |
|---|---|---|
| 0.1 | 0.172 8 | 0.183 2 |
| 1 | 0.172 9 | 0.204 9 |
| 2 | 0.172 0 | 0.332 4 |

Through the analysis of the above data, the PFDL-MFAC algorithm cannot stably track the desired path in data dropout, and the error gradu0ally increases as the data loss rate increases. DC-EMFAC algorithm can effectively predict the system state, the control effect does not deteriorate significantly, and the effect is very ideal.

## 3.3 Different longitudinal speed impact on algorithm performance

Considering that changes in vehicle longitudinal speed can also affect the effectiveness of lateral path tracking, three sets of lateral tracking comparative experiments with different speeds will be conducted to simulate and verify the proposed algorithm with a data packet loss rate of 1%.

The experimental plan is shown in Table 5, and the experimental results are shown in Figure 8. Through analysis, it is not difficult to find that as the longitudinal velocity increases, the system error gradually increases, but it can still track the desired path well.

**Table 5　Different longitudinal speeds**

| | Parameter | Speed |
|---|---|---|
| Scenario 1 | $\eta=1,\ \mu=0.1,\ \lambda=1,$ | 20 km/h |
| Scenario 2 | $\rho_i=[1,0.4,0.6,0.2],\ \xi=4$ | 30 km/h |
| Scenario 3 | | 40 km/h |

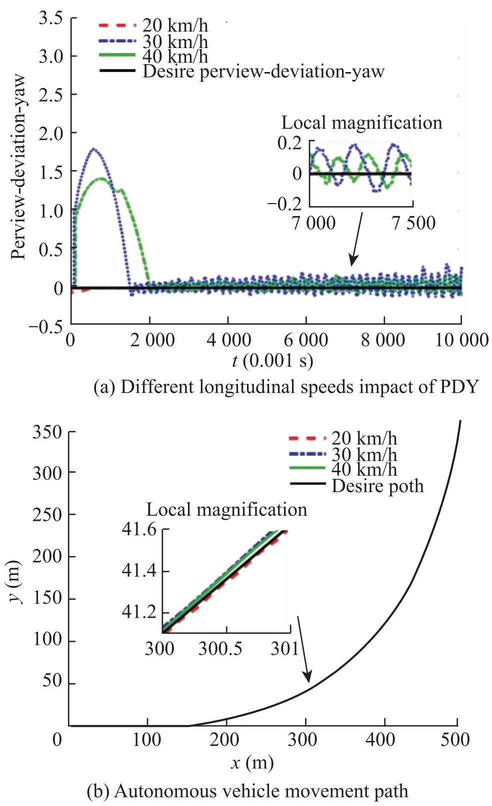

(a) Different longitudinal speeds impact of PDY

(b) Autonomous vehicle movement path

**Fig. 8　Simulations data**

## 4　Conclusion

This paper proposed a DC-EMFAC algorithm to solve the lateral path tracking control problem of autonomous vehicle under data dropout. This algorithm is a data-driven control method which does not require modeling the system, and use the time-varying factor of PG, which greatly optimizes the selection of parameters in the control algorithm. To address the issue of data loss, the missing data is compensated and incorporated into the design of the controller, ensuring the system's normal operation during these scenarios. The feasibility of DC-EMFAC is verified by simulation conducted jointly in Panosim and MATLAB2018b.

## Acknowledgments

This paper is supported by the Beijing Nature Fund (412035 and 4222045), the China Nature Fund (62173002), the North China Institute of Science and Technology Scientific Research Fund, and the North China Institute of Science and Technology Talent Training Project. This project is a special fund of the General Scientific Research Program (KM201911232015) of the Beijing Municipal Education Commission. R&D Program of the Beijing Municipal Education Commission (KM202310009010 and KM202210009011).

## Declaration of competing interest

The authors have no competing interests to declare that are relevant to the content of this article.

## References

[1] SHEN D, ZHANG C, XU Y. Two Updating Schemes of Iterative Learning Control for Networked Control Systems with Random Data Dropouts [J]. Information Sciences, 2017, 381: 352-370.

[2] GE C, YANG L, ZHAO Z W, et al. Stochastic Switched Sampled-Data Control for Uncertain Fuzzy Systems with Packet Dropout [J]. International Journal of Fuzzy Systems, 2021, 23 (1): 145-157.

[3] WANG R R, JING H, HU C, et al. Robust H-infinity Path Following Control for Autonomous Ground Vehicles With Delay and Data Dropout [J]. IEEE Transactions on Intelligent Transportation Systems, 2016, 17 (7): 2042-2050.

[4] LIU S D, HOU Z S, TIAN T T, et al. A Novel Dual Successive Projection-Based Model-Free Adaptive Control Method and Application to an Autonomous Car [J]. IEEE Transactions on Neural Networks and Learning Systems, 2019, 30 (11): 3444-3457.

[5] HOU Z S, BU X H. Model Free Adaptive Control with Data Dropouts [J]. Expert Systems with Applications, 2011, 38 (8): 10709-10717.

[6] WANG Q, JIN S T, HOU Z S. Compensation-Based Co-

operative MFAILC for Multiple Subway Trains Under Asynchronous Data Dropouts [J]. IEEE Transactions on Intelligent Transportation Systems, 2022, 23 (12): 23750-23760.

[7] LUCIANI S, BONFITTO A, AMATI N, et al. Model Predictive Control for Comfort Optimization in Assisted and Driverless Vehicles [J]. Advances in Mechanical Engineering, 2020, 12 (11): 1-14.

[8] ZHANG W. A Robust Lateral Tracking Control Strategy for Autonomous Driving Vehicles [J]. Mechanical Systems and Signal Processing, 2021, 150: 107238.

[9] LIU S, HOU Z, TIAN T, et al. Path Tracking Control of a Self-Driving Wheel Excavator via an Enhanced Data-driven Model-Free Adaptive Control Approach [J]. Iet Control Theory and Applications, 2020, 14 (2): 220-232.

[10] FALCONE P, BORRELLI F, ASGARI J, et al. Predictive Active Steering Control for Autonomous Vehicle Systems [J]. IEEE Transactions on Control Systems Technology, 2007, 15 (3): 566-580.

[11] HOU Z S, JIN S T. A Novel Data-Driven Control Approach for a Class of Discrete-Time Nonlinear Systems [J]. IEEE Transactions on Control Systems Technology, 2011, 19 (6): 1549-1558.

[12] LIN N, CHI R H, HUANG B A. Event-Triggered Model-Free Adaptive Control [J]. IEEE Transactions on Systems Man Cybernetics-Systems, 2021, 51 (6): 3358-3369.

[13] HOU Z S, WANG Z. From Model-based Control to Data-Driven Control: Survey, Classification and Perspective [J]. Information Sciences, 2013, 235: 3-35.

[14] LI X Q, XU Z G. Pattern-Moving-Based Partial Form Dynamic Linearization Model Free Adaptive Control for a Class of Nonlinear Systems [J]. Actuators, 2021, 10: 223-243.

[15] BU X H, YU F S, HOU Z S, et al. Model-Free Adaptive Control Algorithm with Data Dropout Compensation [J]. Mathematical Problems in Engineering, 2012, 2012 (1): 1-14.

[16] ZHU B, LIU Z P, ZHAO J, et al. Driver Behavior Characteristics Identification Strategies Based on Bionic Intelligent Algorithms [J]. IEEE Transactions on Human-Machine Systems, 2018, 48 (6): 572-581.

[17] PAN F, BAO H. Preceding Vehicle Following Algorithm with Human Driving Characteristics [J]. Proceedings of the Institution of Mechanical Engineers Part D-Journal of Automobile Engineering, 2021, 235 (7): 1825-1834.